



The effect of wettability on capillary trapping in carbonates



Nayef Alyafei*, Martin J. Blunt

Qatar Carbonates and Carbon Storage Research Centre, Department of Earth Science and Engineering, Imperial College London, SW7 2AZ, United Kingdom

ARTICLE INFO

Article history:

Received 29 July 2015

Revised 1 February 2016

Accepted 1 February 2016

Available online 23 February 2016

Keywords:

Wettability

Geological CO₂ sequestration

Improved Oil recovery

Capillary trapping

Waterflooding

ABSTRACT

We use an organic acid (cyclohexanepentanoic acid) to alter the wettability of three carbonates: Estailades, Ketton and Portland limestones, and observe the relationship between the initial oil saturation and the residual saturation. We take cores containing oil and a specified initial water saturation and water-flood until 10 pore volumes have been injected. We record the remaining oil saturation as a function of the amount of water injected. In the water-wet case, with no wettability alteration, we observe, as expected, a monotonic increase in the remaining oil saturation with initial saturation. However, when the wettability is altered, we observe an increase, then a decrease, and finally an increase in the trapping curve for Estailades limestone with a small, but continued, decrease in the remaining saturation as more water is injected. This behavior is indicative of mixed-wet or intermediate-wet conditions, as there is no spontaneous imbibition of oil and water. In contrast, Ketton did not show indications of a significant wettability alteration with a similar observed trapping profile to that observed in the water-wet case. Portland limestone also showed a monotonic increasing trend in remaining saturation with initial saturation but with a higher recovery, and less trapping, than the water-wet case. Again, this is intermediate-wet behavior with no spontaneous imbibition of either oil or water, and slow production of oil after water breakthrough. Finally, we repeat the same experiments but instead we age the three carbonates with a high asphaltenic content and high viscosity crude oil at 70 °C mimicking reservoir conditions. The results show a monotonic increase in residual saturation as a function of initial saturation but with higher recovery than the water-wet cases for Estailades and Portland, with again no indication of wettability alteration for Ketton. We discuss the results in terms of pore-scale recovery process and contact angle hysteresis. In these experiments, water-saturated micro-porosity appears to protect the solid surfaces from a strong wettability alteration, particularly in Ketton.

© 2016 Elsevier Ltd. All rights reserved.

1. Introduction

Understanding wettability and its influence on capillary trapping is a key factor in estimating storage and recovery efficiencies. Studies on Carbon Capture and Storage (CCS) and Improved Oil Recovery (IOR) have different emphasis; in CCS residual trapping increases storage security, while for IOR it limits oil recovery. Pore structure and wettability are two of the main factors affecting capillary trapping. Several studies have discussed the trapping curve, which is the relationship between the initial non-wetting phase saturation (S_{nwi}) and the residual non-wetting phase saturation (S_{nwr}), in water-wet media. Fig. 1 shows a selected literature survey of trapping curves of water-wet rocks while Table 1 shows further details of these studies. The main point is that all the studies show a monotonic increase in the residual saturation as a function

of initial saturation: the more non-wetting phase that is initially present, the more that can be trapped. However, the data points do not collapse in one curve and vary, due to different rock types, different fluid properties, and different experimental conditions.

In water-wet rocks, the final, or true residual saturation is reached in these experiments, since trapping is principally caused at the pore scale by snap-off with little oil production after water breakthrough [26,27]. In addition, the increasing trend between initial and residual saturations can be explained since snap-off will render more non-wetting phase immobile if there is more non-wetting phase in the system [24].

We see qualitatively similar trapping curves for both sandstones and carbonates. This indicates that the monotonic increasing trend is a property of water-wet rocks regardless of the complexity of the rock's pore structure. The generic similarity of trapping for carbonates and sandstones for CO₂ systems specifically has also been observed in a recent literature review by Krevor et al. [23].

The literature for cores whose wettability has been altered is more limited compared to the water-wet survey. In this paper, we

* Corresponding author at. Department of petroleum Engineering, Texas A&M University at Qatar.

E-mail address: nmalyafei@gmail.com, Nayef.alyafei@qatar.tamu.edu (N. Alyafei).

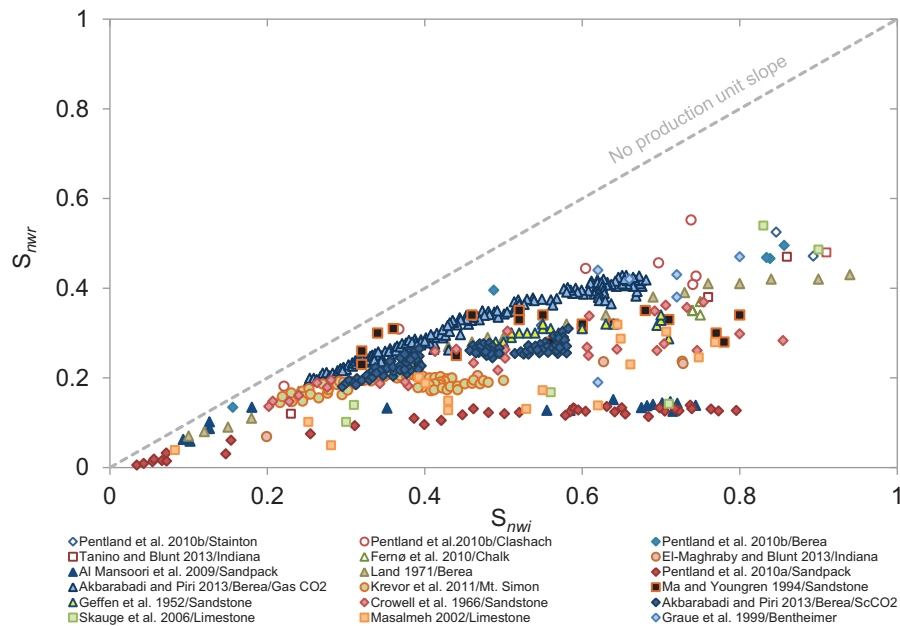


Fig. 1. Literature database of the capillary trapping curve for water-wet porous media.

Table 1

Further information regarding the studies plotted in Fig. 1 for water-wet rocks.

Reference	Rock/type	Fluids
Pentland et al. [38]/Stainton	Stainton/sandstone	n-Decane/brine
Pentland et al. [38]/Clashach	Clashach/sandstone	n-Decane/brine
Pentland et al. [38]/Berea	Berea/sandstone	n-Decane/brine
Tanino and Blunt [47]	Indiana/limestone	n-Decane/brine
Fernø et al. [14]	Chalk/limestone	n-Decane/brine
El-Maghraby and Blunt [13]	Indiana/limestone	CO ₂ /brine
Al Mansoori et al. [3]	Sandpack	Air/brine
Land [25]	Berea/sandstone	N ₂ /oil
Pentland et al. [37]	Sandpack	Octane/brine
Akbarabadi and Piri [1]	Berea/sandstone	Gas CO ₂ /brine
Akbarabadi and Piri [1]	Berea/sandstone	ScCO ₂ /brine
Krevor et al. [22]	Mt. Simon/sandstone	ScCO ₂ /water
Ma and Youngren [28]	Sandstone	Gas/water
Geffen et al. [15]	Sandstone	Gas/water
Crowell et al. [10]	Sandstone	Gas/water
Skauge et al. [44]	Limestone	n-Decane/brine
Masalmeh [31]	Limestone	(Refined oil/n-decane)/brine
Graue et al. [16]	Bentheimer/sandstone	Crude oil/brine

use the term “altered-wettability” to refer to a rock which has been in contact with oil: it may be weakly water-wet, intermediate-wet, mixed-wet, or oil-wet. Fig. 2 shows the trapping curve in altered-wettability porous media and Table 2 shows further details of these studies. In this figure, we do not see a distinct trend compared to water-wet rocks. This can be attributed to the difficulty of reproducing these experiments; since ageing these rocks to establish the wettability depends on the composition of the oil, the experimental conditions, and the rock type. Here we are mixing results from different – often unknown – rock types and wettabilities.

In general though we see less trapping than in water-wet media. This is because, at the pore scale, the oil remains connected in layers for oil-wet and mixed-wet systems and thus low residual saturations may be achieved if sufficient water is injected [43]. For intermediate-wet rocks, where we see local contact angles below 90°, the amount of trapping is controlled by the degree of snap-off: we expect less trapping but a monotonic trend with initial saturation. Furthermore, in many altered wettability samples there is significant, yet slow, oil production after breakthrough

and the “residual” saturation reported may simply be the remaining value at the end of the experiment, rather than a true end point.

Another important feature observed by Tanino and Blunt [47] is a non-monotonic trend of residual saturation with initial saturation. For oil-wet and mixed-wet media, with oil layers, the amount of trapping is controlled by when these layers collapse: layers are more stable for a higher initial oil saturation, leading to less trapping, as we discuss later.

In this paper, we perform waterflood experiments at ambient conditions, and at elevated temperatures on three carbonate rocks at water-wet and altered-wettability conditions. The rocks are 38 mm in diameter and 76 mm in length. We use 1.5 wt% of cyclohexanepentanoic acid in n-decane to alter the wettability into a more oil-wet state. This organic acid is reported in the literature to be a fast way to alter the wettability of calcite and it is commercially available [52].

We use both the porous plate technique and the unsteady state (USS) method to establish different initial oil saturations. We waterflood subsequently to find the residual oil saturation.

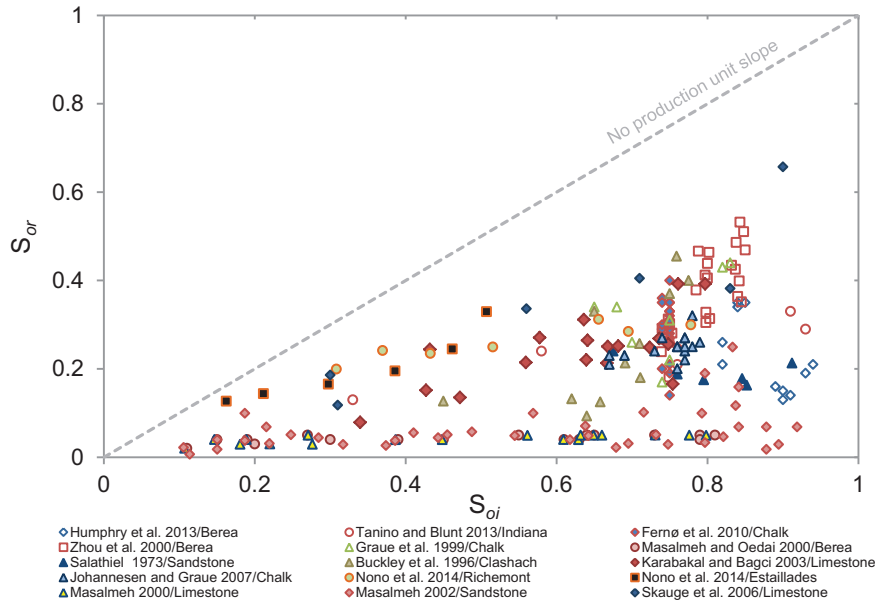


Fig. 2. Literature database of the capillary trapping curve for altered-wettability porous media.

Table 2

Further information regarding the studies plotted in Fig. 2 for altered-wettability rocks.

Reference	Rock/Type	Ageing fluid
Humphry et al. [17]	Berea/sandstone	Crude oil
Tanino and Blunt [47]	Indiana/limestone	Organic acid
Fernø et al. [14]	Chalk/limestone	Crude oil
Zhou et al. [53]	Berea/sandstone	Crude oil
Graue et al. [16]	Chalk/limestone	Crude oil
Masalmeh and Oedai [30]	Berea/sandstone	Crude oil
Salathiel [43]	Sandstone	Crude oil
Buckley et al. [7]	Clashach/sandstone	Crude oil
Karanakal and Bagci [20]	Limestone	Mineral oil
Johannesen and Graue [19]	Chalk/limestone	Crude oil
Nono et al. [35]	Richemont/limestone	Crude oil
Nono et al. [35]	Estailades/limestone	Crude oil
Masalmeh [29]	Limestone	Crude oil
Masalmeh [31]	Sandstone	Crude oil
Skauge et al. [44]	Limestone	Crude oil

For the experiments conducted at elevated temperatures, we use a crude oil with a high asphaltenic content and high viscosity. We age at a temperature of 70°C to alter the wettability and establish the initial oil saturation. Again, we use the porous plate and USS methods to establish a wide range of initial oil saturations before waterflooding.

2. Rocks

We use three different types of carbonate rock in our study. Estailades is an upper cretaceous bioclastic limestone from France, which contains 99% calcite (CaCO_3) and traces of dolomite and silica [51]. The porosity (ϕ) of Estailades ranges from 26.2 to 28.4% based on thirteen direct measurements on the cores used in this study, while the permeability (k) is $1.22\text{--}3.26 \times 10^{-13} \text{ m}^2$. Ketton is an oolitic limestone from the UK which is 99.1% calcite and 0.9 quartz [34]. The porosity ranges from 20.2 to 22.6% and the permeability from 1.07 to $3.55 \times 10^{-12} \text{ m}^2$ based on eight measurements. Portland is a skeletal-peloidal limestone of 96.6% calcite and 3.4% quartz from the UK [6]. The porosity ranges from 17.0 to 22.8% and the permeability from 1.9 to $13 \times 10^{-15} \text{ m}^2$ from 12 measurements.

From a mercury injection test, we can relate the capillary pressure $P_c(S_w)$ to the pore size distribution.

$$r_p = \frac{2\sigma \cos \theta}{P_c(S_w)} \quad (1)$$

This can be further interpreted by using the probability distribution function (f) of a pore entry radius (r_p) [11]:

$$r_p f(r_p) = r_p \frac{dS_w}{dr_p} = -P_c \frac{dS_w}{dP_c} = -\frac{dS_w}{d \ln P_c} \quad (2)$$

assuming invasion of an approximately circular pore of radius r_p . This is an approximate relation as it assumes that the pores are circular in cross-section and assigns all the change in saturation to that pore size.

Fig. 3 shows the measured mercury injection capillary pressure (MICP) of the three rocks (Autopore IV 9520, Weatherford Laboratories, East Grinstead, UK). We can see that Portland has the highest capillary entry pressure (minimum value of $P/2\sigma \cos \theta$ taking $2\sigma \cos \theta = 735.4 \text{ mN/m}^{-1}$) of approximately $0.18 \mu\text{m}^{-1}$ and equivalent r_p , Eq. (1), of $5.6 \mu\text{m}$, while Estailades has a lower capillary entry pressure of approximately $0.029 \mu\text{m}^{-1}$ and equivalent r_p of $35 \mu\text{m}$. Ketton has the lowest capillary entry pressure of approximately $0.017 \mu\text{m}^{-1}$ and equivalent r_p of $59 \mu\text{m}$.

Fig. 4 shows the pore size distribution: we can see that both Estailades and Ketton have distinct bi-modal distributions with at least 50% of pore sizes greater than $0.5 \mu\text{m}$. Portland has a uni-modal distribution with the majority of the pore sizes less than $0.5 \mu\text{m}$.

If we consider $r_p = 0.5 \mu\text{m}$ as the cut off value between micro and macro-porosity, then 35%, 44%, and 81% of Estailades, Ketton, and Portland respectively is micro-porosity. Overall, Fig. 4 shows that these limestone samples have a wide range of estimated pore size: a range that is typically much larger than in sandstones. Estailades and Ketton show clear bi-modal behavior associated with inter and intra-granular porosity, while Portland displays a very wide but uni-modal distribution of pore size.

3. Experimental procedure

In this section, we present detailed information regarding the experimental conditions, apparatus, and procedure used in this study.

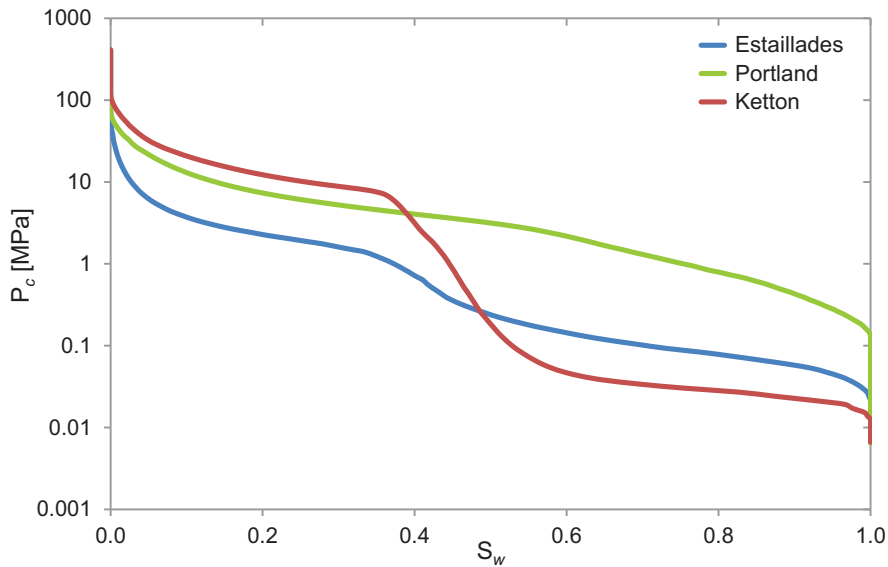


Fig. 3. Measured capillary pressure (mercury/air) as a function of equivalent water saturation.

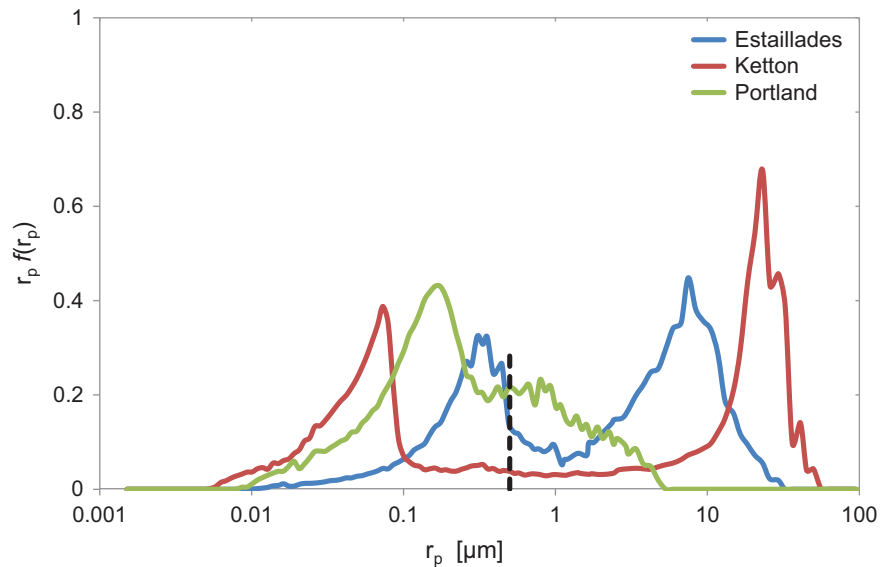


Fig. 4. The pore size distribution against pore throat radius for the three carbonates. The dashed line depicts $r_p = 0.5 \mu\text{m}$.

3.1. Ambient condition waterflooding

3.1.1. Core and brine preparation

- Measure the dimensions and the mass of the dry core.
- Prepare brine of 5 wt% NaCl and 1 wt% KCl with a molality of 1.05 mol kg^{-1} .
- Add smaller samples of the carbonate rock to the mixing of the brine to establish chemical equilibrium between the brine and rock and eliminate any further reaction with the rock.
- Mix the brine for 48 h and leave it to equilibrate for 4 days.
- After that, filter the brine using very fine filter papers.
- After preparing both the core and brine, insert the core into a Hassler cell and vacuum for 12 h.
- In parallel, insert the brine into a vacuum chamber and vacuum for 3–5 h and vacuum saturate the porous plate. This step saves time while saturating the core with brine (primary brine saturation) as the porous plate has a very low permeability.

3.2. Water-wet scenario

3.2.1. Brine saturation

- Inject several pore volumes, PV, of degassed brine into the core at an average flow rate of 2 ml/min, using a Teledyne pump, ISCO 1000D or 500D, until no changes in the differential pressure readings are observed.
- Decrease the pore pressure slowly to atmospheric pressure and then decrease the confining pressure to atmospheric pressure as well.
- Extract the core and weigh it in a beaker filled with degassed brine using a balance with 0.001 g accuracy.
- Insert the core back into the Hassler cell and also insert the brine saturated porous plate in the downstream part of the core.
- To ensure a continuous flow between the core and the porous plate, insert a filter paper between them that will block any

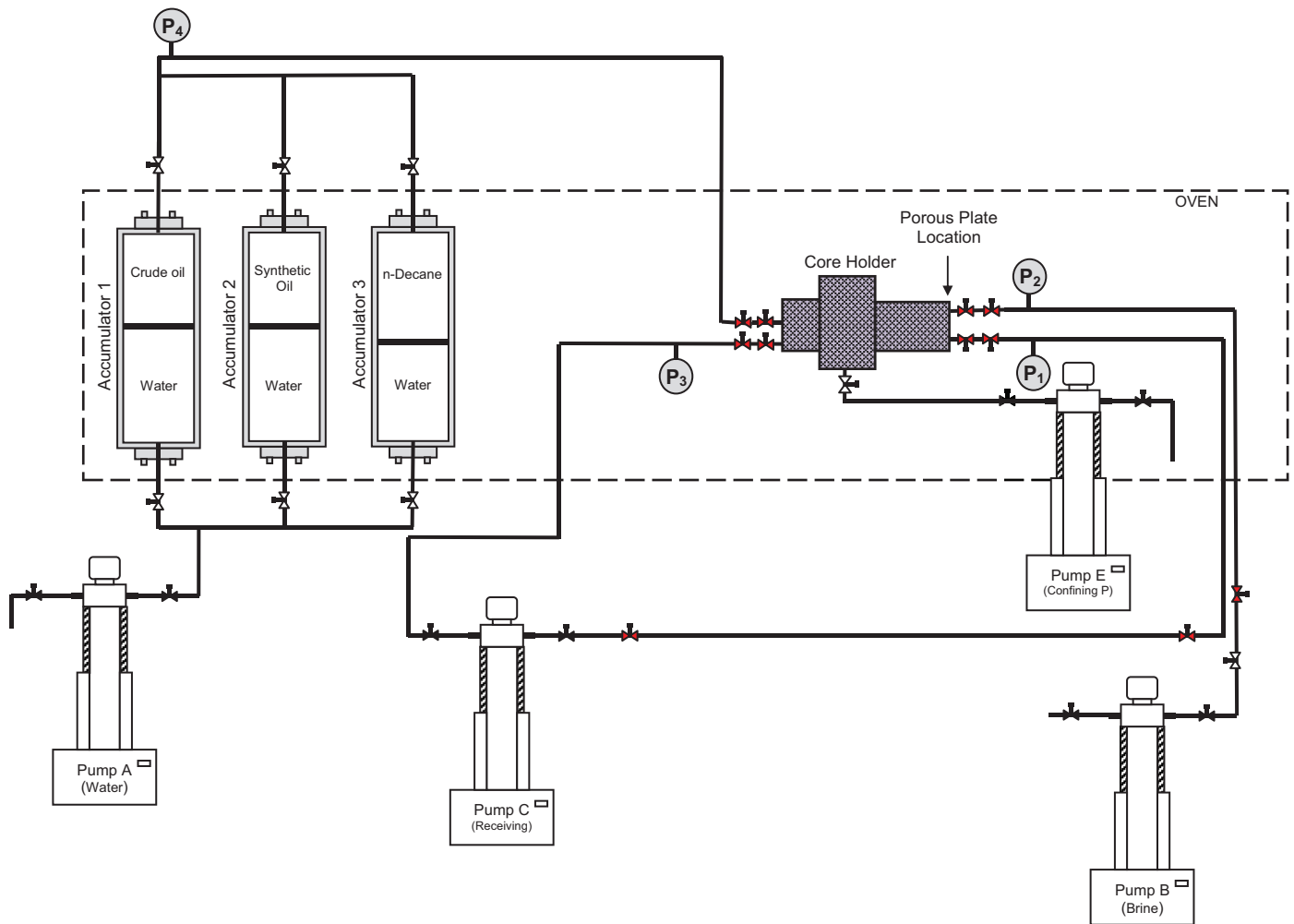


Fig. 5. Schematic of the apparatus used for the coreflood experiments at elevated temperatures.

disintegrated particle from the core to enter the porous plate and hence block it.

- Inject 5 PV of degassed brine.
- The injection scheme should be at a constant differential pressure mode and set the pressure to be slightly lower than the porous plate's differential pressure. Since there are three different types of porous plates (1, 5, and 15 bar; 1 bar $\approx 10^5$ Pa), set the pressures accordingly.
- All the experiments can be performed with the 15 bar porous plate; however, it will take a longer period of time to displace the brine through it as it is the least permeable but can sustain higher pressures. The other two porous plates are more permeable but they cannot sustain more than their intended pressures or they will let air through. For example, using a 5 bar porous plate for a 4 bar differential pressure will take less time to reach equilibrium than using a 15 bar porous plate.
- After fully injecting the 5 PV, seal the core holder to start primary drainage.

3.2.2. Primary drainage

- Inject n-decane (non-wetting phase, Sigma Aldrich, purity $\geq 99\%$) at a constant pressure from the upstream end. The porous plate will retain the n-decane and maintain a fixed brine pressure downstream. The difference between the upstream and the downstream pressures is the capillary pressure. The selection of the capillary pressure depends on the mercury capillary pressure data, Fig. 5. In brief, select capillary pressures in the

transition zone to give different initial oil saturations inside the core.

- Keep track of the differential pressure from the pressure transducers upstream and downstream, as well as the volume of n-decane injected from the pump and the amount of water produced.
- The drainage process ends when there is no further decrease in the volume of n-decane inside the pump is observed and no change in the volume of the brine effluent is detected. Normally, the drainage process takes from 3 days up to 20 days depending on the permeability of the rock and the capillary pressure selected. Higher permeability rocks take less time to reach capillary equilibrium since it is faster for the non-wetting phase to access the rock. Furthermore, low capillary pressures take less time to reach to capillary equilibrium as they access the larger, more permeable, portions of the rock.
- In order to drain the core with the USS method, follow the same procedure as before but do not insert the porous plate and instead inject the n-decane at a constant flow rate for several PVs until the differential pressure across the core becomes constant.

3.2.3. Spontaneous water imbibition

- Take the core out; however, first reduce the pore pressure and then the confining pressure to atmospheric pressure.
- Remove the core and weigh it and then insert it into an Amott cell [4].

- Fill the base part of the Amott cell by one third of degassed brine.
- Seal the Amott cell and open the top part and keep injecting degassed brine until the volume reaches the full minus 1–2 ml.
- Monitor the spontaneous water imbibition until no further n-decane is produced at the top of the cell.
- Take the core out and weigh it and re-insert it back in the core holder for waterflooding.

3.2.4. Waterflooding (forced water injection)

- Apply a confining pressure and inject 5–10 PV of degassed brine until the residual oil saturation is reached. More precisely, this is the oil saturation remaining at the end of injection and may not be the true residual, reached after an infinite amount of waterflooding in systems with an altered wettability. This subtlety is discussed later. The injected flow rate is 0.1 ml/min which represents a capillary number of 3.0×10^{-8} , which is in the capillary-controlled regime [9,40].
- Monitor the amount of n-decane produced after finishing the experiment to find the residual saturation.

3.2.5. Altered-wettability scenario

To alter the wettability of the rock at ambient conditions, we add 1.5 wt% of cyclohexanepentanoic acid (Sigma Aldrich, purity = 98%) in n-decane which we refer to as fluid A. The procedure for the altered-wettability coreflooding experiments is exactly the same as the water-wet experiments discussed above; however, the only differences are that instead of injecting pure n-decane, we inject fluid A, place the altered core in the Amott cell for a duration of 30 days or more, and waterflood the core with 10 PV of brine. We hypothesize that only those surfaces contacted by the initial oil saturation have an altered wettability.

The selected drainage capillary pressure ranges from 30 to 1200 kPa for all the rocks to cover a range of initial oil saturations.

We also notice that the addition of 1.5 wt% of cyclohexanepentanoic acid in n-decane to alter the wettability artificially without crude oil sometimes ages the porous plate to oil-wet conditions allowing oil production from the downstream end. These experiments are excluded in this study.

The waterflood starts at 0.1 ml/min for the first 2 PV and then we increase the flow rate gradually to reach 30 ml/min for Estailades and Ketton. However, for Portland we inject up to a rate of 0.35 ml/min since it has a very low permeability and increasing the flow rate will build up the pressure too high to be able to confine the fluids easily. Masalmeh [32] showed that injecting many PVs at low rate does not lead to better estimation of S_{or} for oil-wet or mixed-wet rocks; the suggested method to get to S_{or} is to increase the rate to overcome the capillary end effect. In our experiments, with a porous plate, increasing the flow rate imposes a large and negative capillary pressure across the sample, driving the system close to the residual saturation. This is consistent with studies employing a constant flow rate, where 10 PV is insufficient to reach the residual oil saturation in altered-wettability rocks [18,43,47]. In contrast, as proposed by Tang and Firoozabadi [45], increasing the imposed pressure gradient will substantially increase the oil recovery.

The fluid properties used in this study are shown in Table 3. We measure the n-decane/brine and fluid A/brine intrinsic contact angles on smooth calcite surfaces by using Ramé-Hart model 590 device. We submerge the calcite crystals in fluid A to alter the surface wettability of the calcite and then we measure the contact angle. In addition, we measure the density and viscosity of the fluids at 20°C using Anton Paar DMA5000 M and Rheotek U-tube viscometer, respectively.

Table 3

Properties of the oil phase fluids used in this study at ambient conditions.

Fluid	ρ [kg/m ³]	μ [mPa s]	σ [mN/m]	θ_1 [deg.]
n-Decane	728.8 ± 0.02	0.92	52.3 ± 0.4 ^a	37.9 ± 2
A	731.5 ± 0.02	0.91	27.52 ± 0.08 ^a	130 ± 3
Mercury	–	–	480	40

^a Measured on the same fluid pairs as the ones used in this paper [47].

3.3. High temperature waterflooding

Fig. 5 shows a diagram of the apparatus used.

3.3.1. Core and fluid preparation

- Vacuum the core for 12 h while the oven which contains the cell heats to 70°C.
- Prepare the brine of 5 wt% NaCl and 1 wt% KCl with a molality of 1.05 mol kg⁻¹ and mix it with smaller pieces of each rock. This mixing happens at 70 °C; smaller amounts of CaCO₃ and magnesium carbonate (MgCO₃) have been shown to dissolve at higher temperatures [12].
- Vacuum the brine for 12 h in a vacuum oven at 70°C. The density of brine at 70°C is reported as 1018 kg/m³ [2].
- Vacuum saturate both the core and the porous plate inside the vacuum oven for 12 h and then weigh the core before inserting it into the Hassler cell.
- Inject 5 PV of heated brine into the core. All the pumps are heated to 70°C using a water bath and heating jackets and the tubes connected to the cell from outside the oven are covered with heating insulation.
- Fill the pump with crude oil and leave it for 6 h before starting the injection in order for the crude oil properties to settle at 70°C.

Table 4 shows the composition of the crude oil and Table 5 shows the properties of the crude oil and n-decane at 70°C; these measurements were provided by Shell Rijswijk, Netherlands, along with the crude oil.

3.3.2. Water-wet scenario

We use the same water-wet trapping data as the ambient conditions data as we do not expect to see significant differences between the results at ambient conditions and 70°C [38,39].

3.4. Altered-wettability scenario

3.4.1. Primary drainage

- When the system is in thermal equilibrium, inject the crude oil from the upstream side of the Hassler cell and collect the brine effluent outside the oven at ambient conditions to avoid evaporation inside the oven. Depending on the capillary pressure injected, the time of this experiment varies. Since the brine effluent is outside the oven, careful monitoring of the amount of brine displaced is possible.
- When no change in the volumes of the injection pump and the effluent are observed, we know that the drainage process has ended.
- Take the core out and weigh it and place it in a container filled with the same crude oil for 40 days for further ageing.
- After that, continuously inject 5 PV of decahydronaphthalene (decalin) and followed by 5 PV of n-decane. Inject the decalin in order to prevent any mixing of n-decane with crude oil which

Table 4
Composition and properties of the crude oil used in this study.

TBN [mg KOH/g oil]	TAN [mg KOH/g oil]	API° [API]	SARA analysis [wt%]			
			Saturates	Aromatics	Resins	Asphaltenes
2.02	0.35	27.8	31.57	50.69	14.29	3.46

Table 5
Fluid properties of the n-decane and the crude oil used in this study at 70°C.

Fluid	ρ [kg/m ³]	μ [mPa s]	σ [mN/m]	θ_I [deg.]	θ_A [deg.]	θ_R [deg.]
n-Decane	691 ^a	0.49 ^a	40.0 ^a	–	–	–
Crude oil	856	6.51	27.2 ^b	100 ^b	81 ^b	109 ^b

^a For μ and ρ of n-decane and σ measured with n-decane/synthetic brine (consisting of 10,000 mg/L NaCl, 70 mg/L MgCl₂·6H₂O, and 200 mg/L CaCl₂·2H₂O) fluid pair, all these measurements were performed at 70 °C [17].

^b Measured on a smooth surface with the same crude oil and with brine of 4.39 mol kg⁻¹ molality NaCl at 50 °C and ambient pressure provided by Shell Rijswijk, Netherlands. Note that the measurement was conducted using an oil droplet on a smooth calcite surface through brine thus $\theta_R > \theta_A$.

may lead to asphaltene deposition [8,14,48,50]. In addition, using n-decane will assess the stability of the wettability alteration.

- Extract the core and place it in the Amott cell.
- For the USS method, repeat the same procedure but without the porous plate and inject 5 PV of crude oil at a constant flow rate. Following that, inject 5 PV of decalin and after that 5 PV of n-decane. This method is also referred to as dynamic wettability alteration.

3.4.2. Spontaneous water imbibition

- Insert the core into a half full Amott cell with 70°C degassed brine.
- Top the additional volume of brine from the top of the cell until reaching the full volume minus 2–3 ml.
- Seal the Amott cell but not fully and place it into the oven at the same temperature of 70°C.
- After 30 min, seal the cell perfectly and that step is to avoid any fluid expansion which may lead to pressurization of the cell, and leave it for 30 days.
- Monitor the cell, until no further volume of n-decane is produced.
- Record the final volume of n-decane produced and the weight of the core after spontaneous water imbibition.

3.4.3. Waterflooding

- Place the core again in the Hassler Cell.
- Inject up to 10 PV of degassed brine at 70°C starting from a flow rate of 0.1 ml/min and which gradually increases until a high flow rate is reached as discussed for the ambient condition experiments.
- Monitor the volume of n-decane in the effluent and weigh the core after the injection of the brine for the residual oil saturation measurement.

4. Results and discussion

4.1. Amott wettability indices

4.1.1. Ambient conditions

For the water-wet systems, we see significant recovery from spontaneous water imbibition; the Amott water index, $I_w > 0.9$ for all the rocks, Table 6. For the altered-wettability systems, there is no spontaneous water imbibition, $I_w = 0$ for Estailades and Portland. However, for Ketton, we have $I_w > 0.9$ indicating no sign

of wettability alteration. In Ketton, as we show later, we do not invade the micro-porosity with wettability-altering agent (the oil phase). As a result, we can only saturate the large macro-pores at relatively low capillary pressures with little wettability alteration.

For I_o , we do not see any oil imbibition. A similar behavior have been noticed by Fernø et al. [14] where no oil imbibition occurred when chalk limestones were aged by crude oil, despite a low I_w . This might indicate that the systems are intermediate-wet since the rocks do not imbibe any water: if we consider that the system has an intrinsic contact angle $\theta_I \approx 90^\circ$, then based on Morrow [33] with contact angle hysteresis on a rough surface, we will have an advancing angle in waterflooding $\theta_A > 90^\circ$ while the receding (oil injection) contact angle $\theta_R < 90^\circ$. This means that the medium is non-wetting to both water during waterflooding and oil in oil invasion leading to no spontaneous imbibition of either phase.

4.1.2. Elevated temperatures

For spontaneous water imbibition we see $0.07 > I_w > 0.17$ for Estailades and Portland, Table 7. Ketton shows again $I_w > 0.9$ indicating no sign of wettability alteration. Since the results here showed more recovery from spontaneous imbibition this indicates that the crude oil ageing is weaker than the organic acid, leaving some portions of the pore space water-wet.

Overall, for these rocks and the two wettability-altering agents studied (crude oil and organic acid) the degree of wettability alteration is modest. We study here systems that are more intermediate-wet with little or no spontaneous imbibition of either water or oil, indicating intrinsic contact angles of around 90°.

4.2. Leverett J-function and oil accessibility

4.2.1. Ambient conditions

We compute the Leverett J -function which is written as follows:

$$J(S_w) = \frac{P_c}{\sigma \cos \theta} \sqrt{\frac{k}{\phi}} \quad (3)$$

where $J(S_w)$ is the dimensionless J -function, P_c is capillary pressure [Pa], σ is interfacial tension (0.48 N/m for a mercury/air system), θ is the contact angle (40° for a mercury/air system, measured through air), ϕ is porosity, and k is permeability [m²].

We compare the Leverett J -function from our measured capillary pressures during oil invasion to that derived from the MICP experiments, Fig. 3. For the ambient condition experiments we take ϕ and k from Table 6 and σ of 52.3 mN/m for the n-decane/brine system and 27.52 mN/m for fluid A/brine system, and

Table 6

Detailed summary of the petrophysical properties, capillary trapping data, and Amott water index for the ambient conditions waterflooding experiments. I_o is zero for all the rocks. The data above the dashed line are water-wet data while the ones below it are altered-wettability data. The S_{oi} and S_{or} data are the average of the mass and volume balance methods and the error bars are the standard deviation of these measurements. E, K, and P denote Estailades, Ketton, and Portland, respectively.

Core label	D [mm]	L [mm]	ϕ [%]	k [m ²]	S_{oi}	S_{or}	I_w
E1	37.8	76.51	26.4	2.07×10^{-13}	0.68 ± 0.02	0.34 ± 0.007	0.91
E2	37.88	76.28	27.3	1.69×10^{-13}	0.59 ± 0.04	0.32 ± 0.04	0.96
E3	37.77	76.4	27.8	2.58×10^{-13}	0.53 ± 0.08	0.26 ± 0.03	0.95
E4	37.66	75.81	28.0	2.96×10^{-13}	0.78 ± 0.025	0.45 ± 0.025	0.99
E5	37.82	76.63	26.2	1.94×10^{-13}	0.95 ± 0.045	0.43 ± 0.01	0.96
E6	37.75	76.08	27.2	1.77×10^{-13}	0.86 ± 0.04	0.1 ± 0.05	0
E7	37.79	76.29	27.3	2.03×10^{-13}	0.94 ± 0.05	0.27 ± 0.05	0
E8	37.87	76.22	28.0	2.18×10^{-13}	0.6 ± 0.025	0.22 ± 0.03	0
E9	37.65	76.24	27.9	3.26×10^{-13}	0.67 ± 0.07	0.12 ± 0.02	0
E10 ^a	37.73	76.39	26.8	1.22×10^{-13}	0.58 ± 0.025	0.33 ± 0.04	0
K1 ^a	37.74	76.22	20.2	1.38×10^{-12}	0.68 ± 0.06	0.33 ± 0.05	0.93
K2 ^a	37.87	75.29	22.0	1.07×10^{-12}	0.48 ± 0.08	0.21 ± 0.07	0.95
K3	37.87	75.29	22.0	1.07×10^{-12}	0.61 ± 0.09	0.25 ± 0.08	0.91
K4 ^a	37.9	76.48	21.9	1.28×10^{-12}	0.64 ± 0.05	0.33 ± 0.05	0.93
K5	37.9	76.28	22.0	2.1×10^{-12}	0.36 ± 0.05	0.17 ± 0.05	0.92
K6	37.7	76.23	22.6	3.55×10^{-12}	0.59 ± 0.05	0.3 ± 0.05	0.95
P1	37.85	76.38	22.8	5.24×10^{-15}	0.27 ± 0.03	0.19 ± 0.03	0.9
P2	37.84	76.19	19.7	3.2×10^{-15}	0.4 ± 0.02	0.3 ± 0.02	0.92
P3 ^a	37.95	76.35	19.8	1.9×10^{-15}	0.56 ± 0.03	0.39 ± 0.03	0.93
P4 ^a	37.95	76.25	18.0	1.8×10^{-15}	0.68 ± 0.03	0.44 ± 0.03	0.95
P5	37.89	76.28	18.9	7.2×10^{-15}	0.49 ± 0.09	0.27 ± 0.1	0
P6	37.81	76.35	18.6	4.17×10^{-15}	0.25 ± 0.03	0.16 ± 0.05	0
P7	37.9	76.25	17.0	1.3×10^{-14}	0.38 ± 0.03	0.18 ± 0.06	0
P8 ^a	37.92	76.35	21.0	6.2×10^{-15}	0.38 ± 0.03	0.21 ± 0.03	0

^a Measured using the USS method.

Table 7

Summary of the petrophysical properties, capillary trapping data, and Amott water index for the high temperatures waterflooding experiments for altered-wettability samples. Again, I_o is zero for all the rocks. The S_{oi} and S_{or} data are the average of the mass and volume balance methods and the error bars are the standard deviation of these measurements.

Core label	D [mm]	L [mm]	ϕ [%]	k [m ²]	S_{oi}	S_{or}	I_w
E11	37.65	76.52	26.2	2.25×10^{-13}	0.89 ± 0.05	0.32 ± 0.1	0.12
E12	37.75	76.26	27.6	1.69×10^{-13}	0.65 ± 0.08	0.19 ± 0.12	0.15
E13 ^a	37.65	76.42	28.4	2.06×10^{-13}	0.8 ± 0.05	0.26 ± 0.08	0.07
K7 ^a	37.9	76.48	21.8	1.54×10^{-12}	0.6 ± 0.02	0.33 ± 0.05	0.9
K8	37.9	76.28	22.0	2.6×10^{-12}	0.38 ± 0.05	0.18 ± 0.07	0.92
P9	37.66	76.42	18.5	2.47×10^{-15}	0.83 ± 0.04	0.47 ± 0.05	0.13
P10	37.84	76.09	20.9	9.9×10^{-15}	0.29 ± 0.04	0.12 ± 0.09	0.11
P11	37.73	76.38	19.4	3.57×10^{-15}	0.83 ± 0.06	0.38 ± 0.088	0.09
P12 ^a	37.89	76.21	19.2	5.77×10^{-15}	0.61 ± 0.035	0.25 ± 0.035	0.17

^a Measured using the USS method.

$\theta = 37.9^\circ$ for the two cases, based on our direct contact angle measurements.

Fig. 6 shows the computed Leverett J -function for the three carbonates. The figure indicates that after accounting the contact angle and interfacial tension, the drainage behavior of n-decane is similar to mercury to within experimental error for water-wet data. For the altered-wettability samples, we observe a higher Leverett- J function compared to the water-wet state. This can be attributed to the uncertainty in the interfacial tension as very limited data is available in the literature and the values were not directly measured for this study.

As mentioned previously, the mercury injection curves for Estailades and Ketton indicate a bi-modal pore size distribution (the two regions of relatively low slope on the figure), with a connected macro-porous inter-granular porosity, and intra-granular micro-porosity that is only accessed at high capillary pressures.

For Estailades and Portland at high initial oil saturations, the oil will access the micro-porosity, Fig. 6a and c, respectively. However, for Ketton, Fig. 6b, even with high capillary pressure the oil was not able to access the micro-pores. In Ketton the grains are porous,

which accounts for 40% of the total porosity: if these remain water-saturated after primary drainage, this could protect the large pores between grains from changing their wettability since there is little or no direct contact of oil with the solid surface [21].

4.2.2. Elevated temperatures

Similarly for elevated temperatures, we compare the Leverett J -functions. In this case, we use ϕ and k from Table 7, σ of 27.2 mN/m and $\theta = 37.9^\circ$.

Similar to the ambient conditions, for both Estailades and Portland, Fig. 7a and c respectively, we can access the micro-pores at the selected capillary pressure. However, for Ketton, Fig. 7c, the induced capillary pressure is not sufficient to access the micro-pores which again could be an explanation for the weak wettability alteration in this case.

Pore structure alone seems to influence the degree of wettability alteration in these three calcites: if a significant fraction of the micro-porosity remains water filled, particularly if this micro-porosity is intra-granular, this water appears to protect the larger pores from wettability alteration.

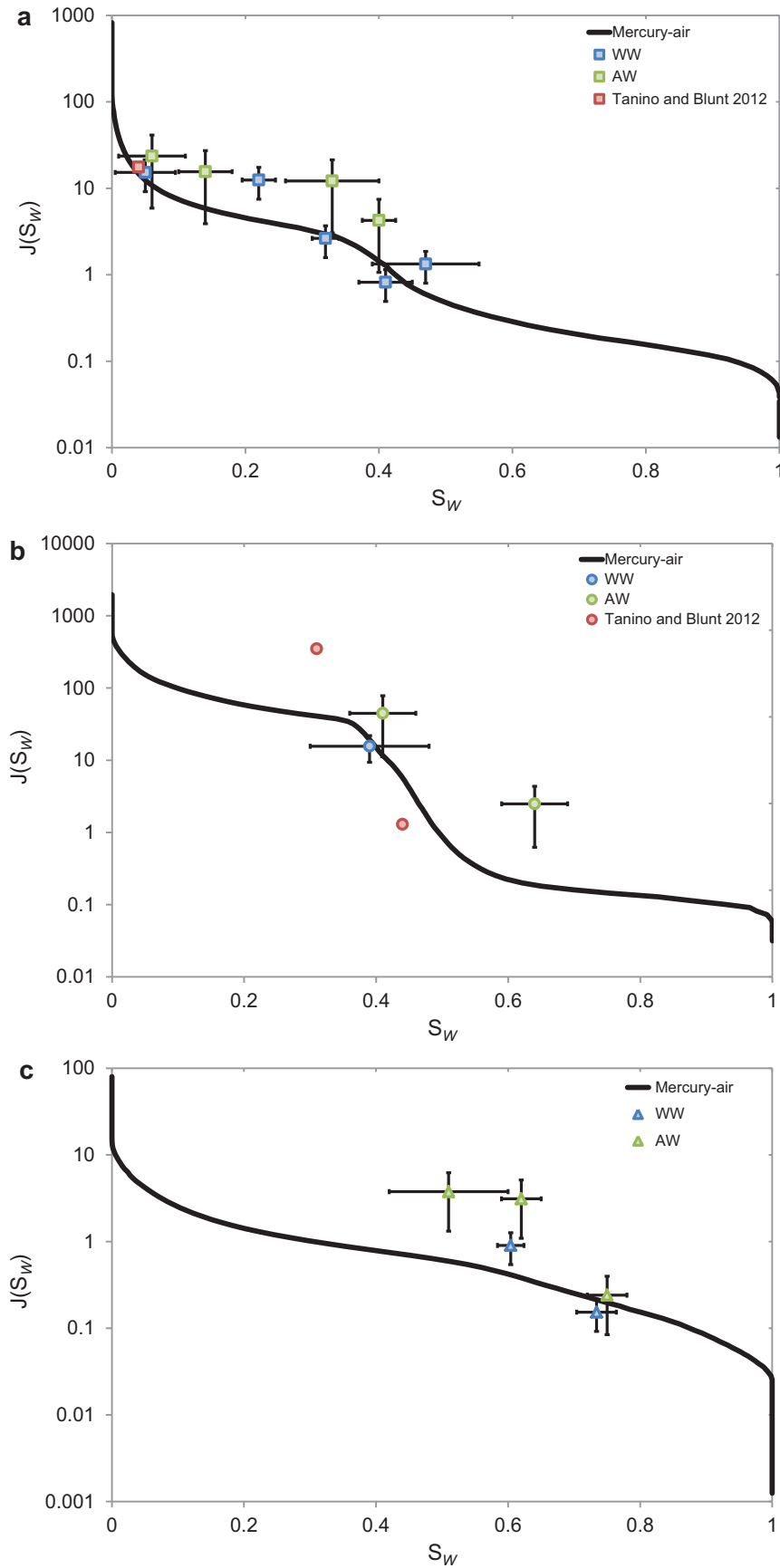


Fig. 6. Leverett J -function, Eq. (3), for ambient conditions experiments and MICP data for (a) Estailades, (b) Ketton, and (c) Portland core samples. In addition, we include water-wet literature data for Estailades and Ketton from Tanino and Blunt [46].

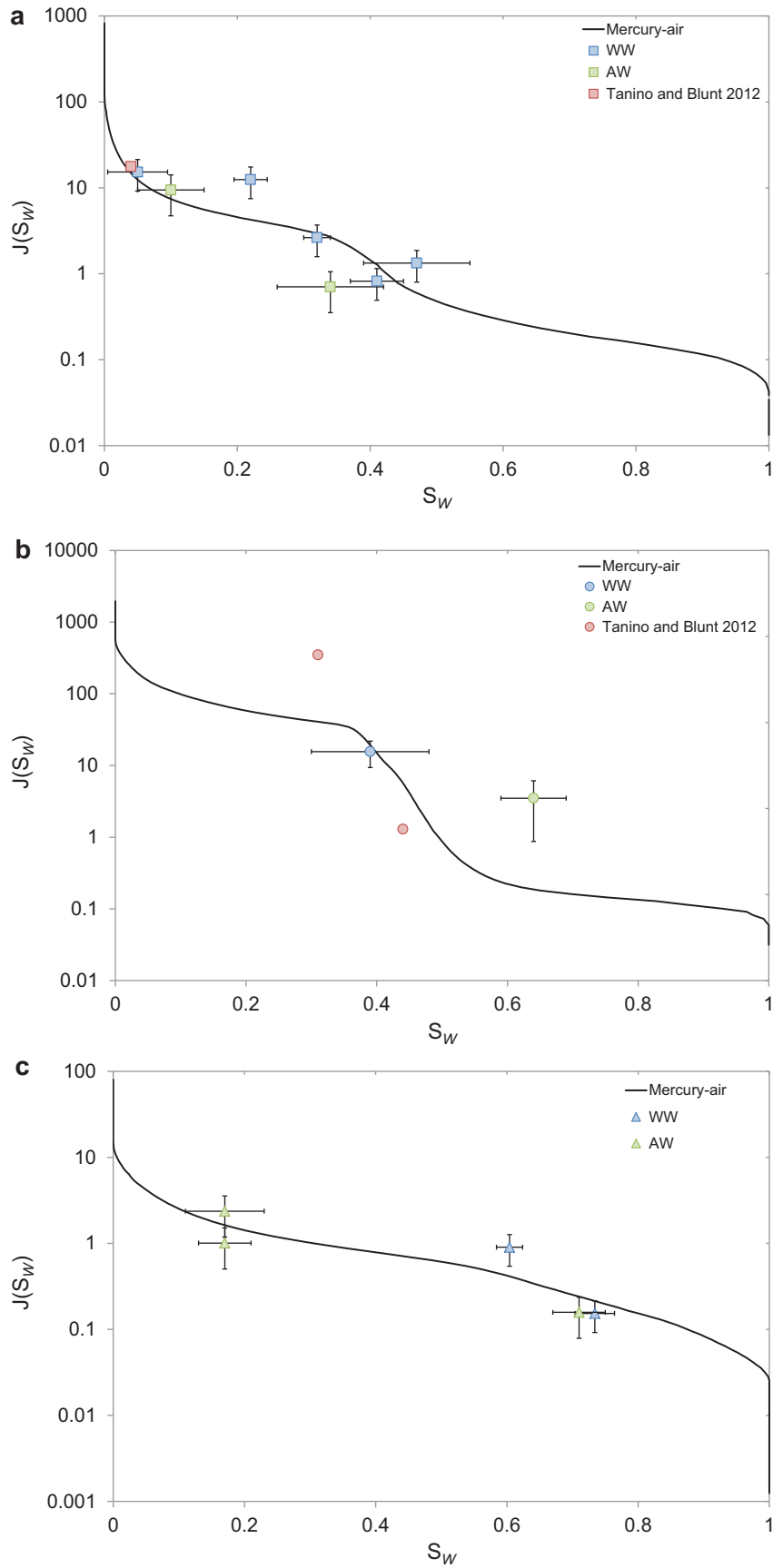


Fig. 7. Leverett J -function, Eq. (3), for elevated temperatures experiments and MICP data for (a) Estailades, (b) Ketton, and (c) Portland core samples. In addition, we include water-wet literature data for Estailades and Ketton from Tanino and Blunt [46].

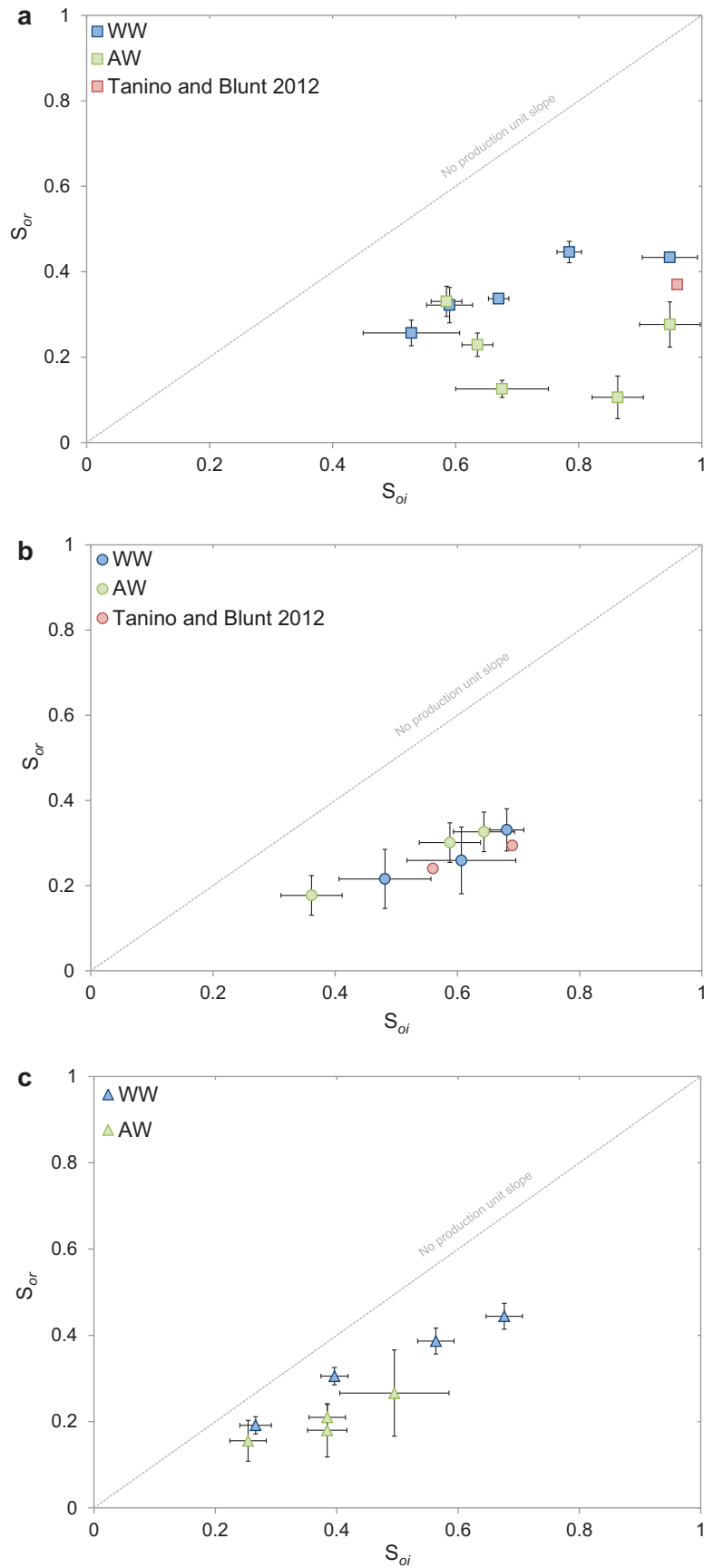


Fig. 8. Remaining oil saturation as a function of initial oil saturation trapping curve at ambient conditions for water-wet and altered-wettability for (a) Estailades, (b) Ketton, and (c) Portland core samples. The data plotted represent an average value of mass balance and volume balance while the error bars represent the standard deviation. In addition, we include water-wet literature data for Estailades and Ketton from Tanino and Blunt [46].

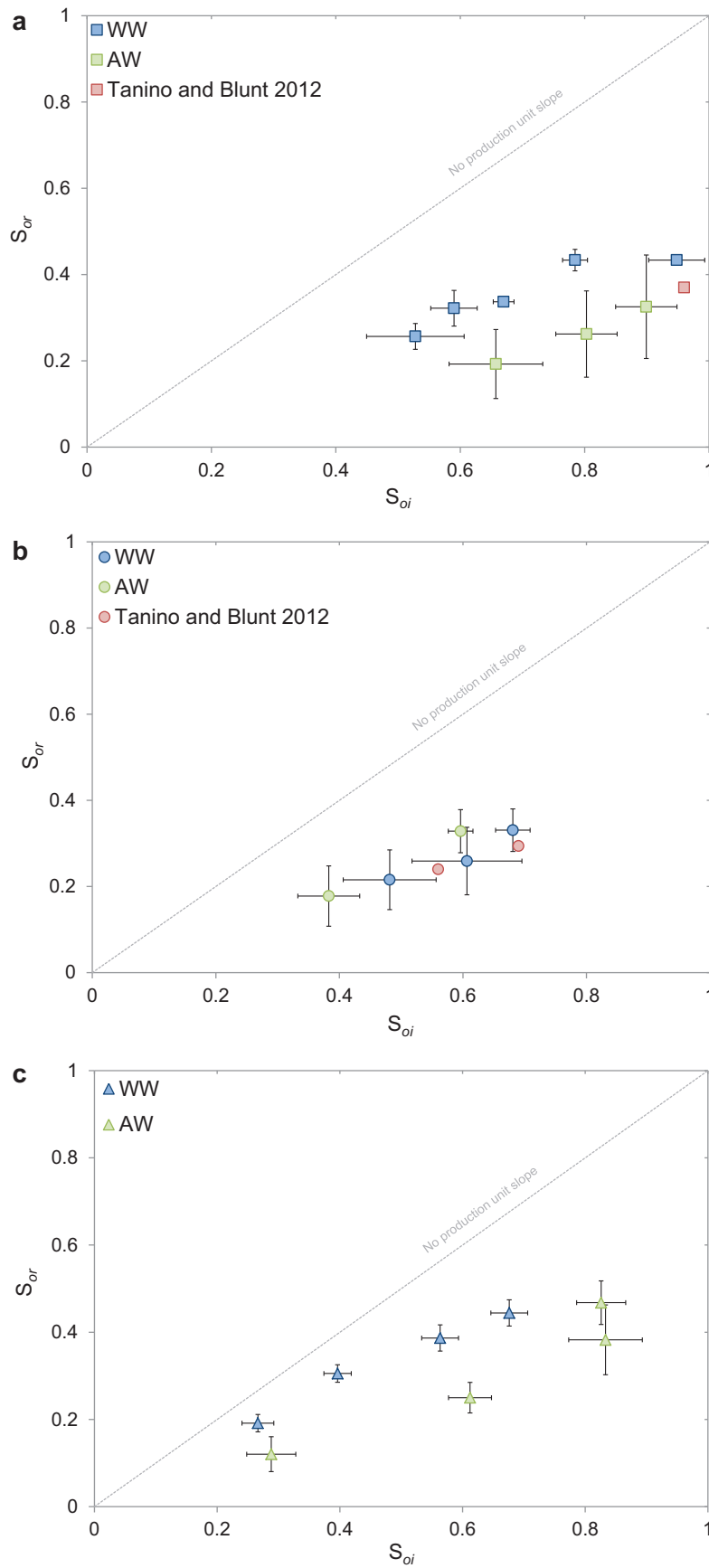


Fig. 9. Remaining oil saturation as a function of initial oil saturation trapping curve at elevated temperatures for water-wet and altered-wettability for (a) Estallades, (b) Ketton, and (c) Portland core samples. The data plotted represent an average value of mass balance and volume balance while the error bars represent the standard deviation. In addition, we include water-wet literature data for Estallades and Ketton from Tanino and Blunt [46].

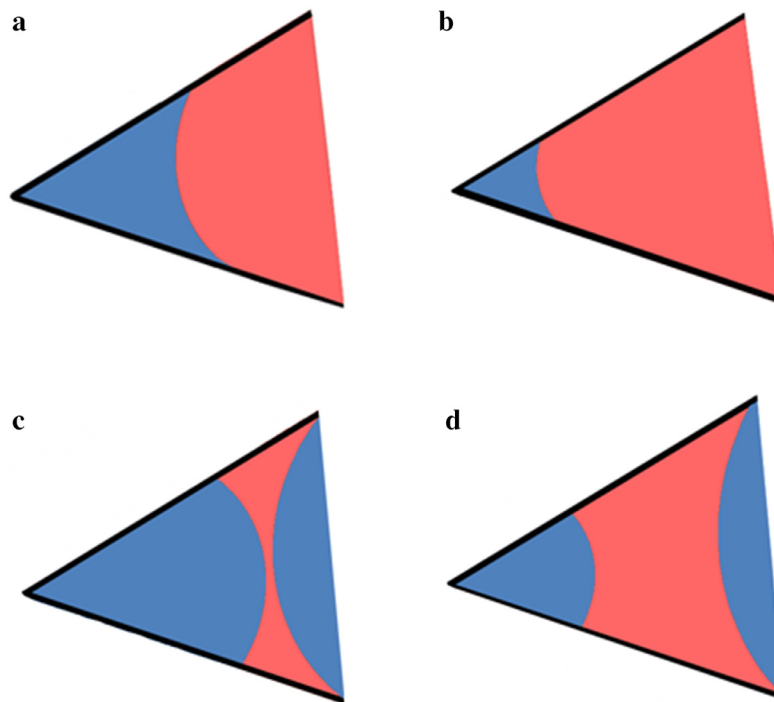


Fig. 10. Schematic of different possible saturation configurations in an oil-wet pore. (a) For a low initial oil saturation (red), after waterflooding (blue) we see a thin oil layer that will collapse with a small increase in water pressure (b). (c) For a high initial oil saturation, in contrast, after waterflooding the oil layer is fatter and more stable (d). (For interpretation of the references to color in this figure legend, the reader is referred to the web version of this article.)

4.3. Trapping curves and waterflood recovery

4.3.1. Organic acid

Fig. 9 shows the water-wet and altered-wettability trapping curve for the three rocks, showing the remaining oil saturation after 10 PV of waterflooding as a function of initial oil saturation. For the water-wet systems, we see a monotonic increase in the trapping curve for all the rocks as expected, since here we see no evidence of a significant change in wettability.

For the altered-wettability systems for Ketton, Fig. 8b, we see a monotonic increase in the trapping curve with no further recovery beyond the first PV injected, as we expected.

For Estailades, Fig. 8a, we notice an unexpected trend in remaining oil saturation with initial saturation with three different regimes. First, we see most trapping for $S_{oi} = 0.58$. Second, we see a decrease in the remaining oil saturation for $0.58 < S_{oi} \leq 0.86$; this can be explained by the stability of oil layers discussed in more detail later. Third, we see an increase again for $S_{oi} > 0.86$: this can be explained by trapping of oil in micro-porosity. This complex trend has been observed previously by Salathiel [43] and Tanino and Blunt [47] in oil-wet and mixed-wet rocks.

For Portland, Fig. 8c, we observe intermediate behavior between Estailades and Ketton where we see a monotonic increase in the trapping curve but with slightly higher recovery, less trapping, than the water-wet case. A similar trend of a monotonic increase in the trapping curve in altered wettability rocks have been observed by Karanakil and Bagci [20] and Nono et al. [35]. This can be explained by the high fraction of micro to macro-porosity in Portland. Portland has the highest fraction of micro-porosity, see Fig. 4, compared to the other rocks. However, these micro-pores are bigger than Ketton's which allows oil to access these pores at a lower capillary pressure. Still, with the selected capillary pressures, not all the pores have been contacted with oil, protecting the surfaces from a strong wettability alteration.

4.3.2. Crude oil

The results using crude oil are illustrated in Fig. 9. For the altered-wettability rocks, we see a monotonic increasing trend but with higher recovery than the water-wet case for Estailades and Portland. For Ketton, we see no sign of wettability alteration and similar trapping to the water-wet cases. Overall, these results are indicative of intermediate-wet behavior with less trapping than for water-wet rocks. This is consistent with the direct contact angle measurements, Table 5.

5. Pore-scale explanation

In this section, we will interpret the results in terms of pore-scale displacement processes. Specifically we will explain trapping for water-wet, intermediate-wet and oil-wet systems in the context of our results.

The water-wet behavior is controlled, at the pore-scale, by snap-off [26,41]. During waterflooding, water fills the narrowest regions of the pore space, stranding oil in the larger pores. This leads to a large residual saturation. S_{or} increases with S_{oi} , as the more of the pore space initially filled, the more oil that can be trapped.

In terms of relative permeability, water is poorly connected, being in the smaller regions of the pore space or in wetting layers, and so is held back, allowing oil to flow readily. The consequence is that during waterflooding, the maximum recovery is seen at, or shortly after, breakthrough. Subsequent water injection does not recover additional oil, as we see in our experiments.

We see water-wet behavior in all our samples without wettability alteration and in Ketton, where the water-filled micro-porosity appears to protect the solid from wettability alteration.

In intermediate-wet media with $\theta \approx 90^\circ$, we see less snap-off. Snap-off becomes less favored compared to direct displacement as the contact angle increases. Direct displacement of oil by water would simply push out the oil with no trapping.

Hence, intermediate-wet systems see lower residual saturations: there is still some trapping by snap-off and bypassing, where a connected front of water simply surrounds the oil [26]. Again, the higher S_{oi} , the more oil that can be trapped and so the trapping curve is monotonically increasing, as in the water-wet case.

In our experiments, intermediate-wet behavior is observed, when crude oil is the wetting agent, in Estailades and Portland. This is consistent with contact angle measurements on smooth calcite, Table 5. While some water is spontaneously imbibed, no oil is imbibed and we do not see the signature of oil layer drainage – very low S_{or} , significant post-breakthrough recovery and non-monotonic trapping curves [43]. Hence, we assume in these cases that we have $\theta_A \approx 90^\circ$. We also see intermediate-wet behavior for Portland with organic acid: here $I_w = I_o = 0$, but the waterflood behavior indicates that the significant water-filled micro-porosity protects to some extent, the surfaces from a stronger wettability change.

We only see oil-wet behavior in one case: Estailades with organic acid. While $I_w = I_o = 0$, we can reach $S_{or} < 0.1$, we see a non-monotonic trapping curve and significant recovery after breakthrough. We now provide a pore-scale explanation for this behavior. The contact angle measurements in Table 3 show that oil-wet conditions are possible in this case.

Fig. 10 shows how—if a pore is oil-wet—water can enter as the non-wetting phase, leaving an oil layer sandwiched between water in the corner and the oil in the center of the pore. These layers keep the oil connected in the pore space, preventing trapping, but have a low conductance, meaning that the oil relative permeability is low [36,42,43,49]. If the initial oil saturation is high, water is squeezed into the corners and the oil layers are thick. As more water is injected and the water pressure increases, the layers will become thinner and, when they collapse, will allow some oil to be trapped. However, as we see, remaining oil saturations of less than 10% are possible. For lower S_{oi} , there is more water in the corners, the layers are thinner and collapse earlier during waterflooding, giving more trapping and a higher S_{or} .

For the very highest values of S_{oi} , however, S_{or} increases again. This is likely due to oil invading micro-porosity in which additional oil may be trapped.

It is interesting that even for the same oil and physical conditions of temperature and pressure, we can observe very distinct behavior for three rocks whose chemical composition (almost pure calcite) are similar: from water-wet behavior in Ketton, to intermediate-wet in Portland, to intermediate to oil-wet in Estailades. This demonstrates the need for good benchmark experiments, as clearly the behavior is dependent to a significant degree on the pore structure. In particular, water-filled micro-porosity appears to protect the solid surfaces from wettability alteration in Ketton and, to a lesser extent, in Portland.

These results also have implications for field-scale recovery in transition zone carbonate reservoirs, where there is a range of initial oil saturation. We suggest that water-wet behavior may be seen where micro-porosity has not been invaded by oil during primary oil migration. Future work could extend these studies to a wider range of rocks, mineralogies and oils, relating our macroscopic measurements with microscopic in situ determination of contact angle [5].

6. Conclusions

We have presented a methodology for the study of capillary trapping in carbonates, combining a reproducible and rapid method for ambient-condition wettability alteration with an organic acid and with a crude oil ageing at high temperature. We see significant recovery by spontaneous imbibition in water-wet rocks, followed by little to no recovery by subsequent waterflooding.

The trapping curve for these rocks increases monotonically with initial saturation, as expected. For altered-wettability rocks, the behavior is more complex.

For Estailades limestone, aged with organic acid, we observe a non-monotonic increase in the trapping curve consistent with oil-wet behavior. When the core is aged with crude oil and replaced with decane, we observe an intermediate-wet behavior, with slightly higher recovery than the water-wet case and a monotonic trapping curve.

For Ketton, we observe a monotonic increase in the trapping curve for both altered-wettability cases. This is explained by the nature of Ketton limestone having significant amount of micro-pores as intra-granular porosity that remain water-saturated and which appear to protect the grains from wettability change.

For Portland, we observe an intermediate case between Estailades and Ketton for both altered-wettability cases with higher recovery than the water-wet case but with a monotonic increase in the trapping curve. This can be explained by the pore structure, since Portland has the highest fraction of micro-porosity compared to the other limestones; however, some of this micro-porosity is accessed during primary drainage, allowing some wettability change.

These results were explained and interpreted in terms of pore-scale displacement processes.

Acknowledgments

We would like to acknowledge funding from the Qatar Carbonates and Carbon Storage Research Centre, QCCSRC, which is supported jointly by Qatar Petroleum, Shell and the Qatar Science & Technology Park (grant no. EAPER/1160).

References

- [1] Akbarabadi M, Piri M. Relative permeability hysteresis and capillary trapping characteristics of supercritical CO₂/brine systems: an experimental study at reservoir conditions. *Adv Water Resour* 2013;52:190–206. <http://dx.doi.org/10.1016/j.advwatres.2012.06.014>.
- [2] Al Ghafri S, Maitland GC, Trusler JPM. Densities of aqueous MgCl₂ (aq), CaCl₂ (aq), KI (aq), NaCl (aq), KCl (aq), AlCl₃ (aq), and (0.964 NaCl+ 0.136 KCl)(aq) at temperatures between (283 and 472) K, pressures up to 68.5 MPa, and molalities up to 6 mol kg⁻¹. *J Chem Eng Data* 2012;57:1288–304. <http://dx.doi.org/10.1021/jje2013704>.
- [3] Al Mansoori S, Iglauer S, Pentland CH, Bijeljic B, Blunt MJ. Measurements of non-wetting phase trapping applied to carbon dioxide storage. *Energy Proc* 2009;1:3173–80. <http://dx.doi.org/10.1016/j.ijggc.2009.09.013>.
- [4] Amott E. Observations relating to the wettability of porous rock. *Trans AIME* 1959;219:156–62.
- [5] Andrew M, Bijeljic B, Blunt MJ. Pore-scale contact angle measurements at reservoir conditions using X-ray microtomography. *Adv Water Resour* 2014;68:24–31. <http://dx.doi.org/10.1016/j.advwatres.2014.02.014>.
- [6] Brechley PJ, Rawson PF. The geology of England and Wales. London: The Geological Society; 2006. <http://dx.doi.org/10.1144/GOEWP>.
- [7] Buckley JS, Bousseau C, Liu Y. Wettability alteration by brine and crude oil: from contact angles to cores. *SPE J* 1996;1:341–50. <http://dx.doi.org/10.2118/30765-PA>.
- [8] Buckley JS, Fan T, Tong Z, Morrow NR. Some mechanisms of crude oil/brine/solid interactions. In: Proceedings of society of core analysts held in Trondheim, Norway, SCA2006-02; 2006.
- [9] Chatzis I, Morrow NR. Correlation of capillary number relationships for sandstone. *SPE J* 1984;24:555–62. <http://dx.doi.org/10.2118/10114-PA>.
- [10] Crowell DC, Dean GW, Loomis AG. Efficiency of gas displacement from a water-drive reservoir. US Dept. of the Interior, Bureau of Mines; 1966.
- [11] Dullien FAL. Porous media: fluid transport and pore structure. New York: Academic Press; 1991. <http://dx.doi.org/10.1016/B978-0-12-223651-8.50001-8>.
- [12] El-Maghraby RM, Pentland CH, Iglauer S, Blunt B. A fast method to equilibrate carbon dioxide with brine at high pressure and elevated temperature including solubility measurements. *J Supercrit Fluids* 2012;62:55–9. <http://dx.doi.org/10.1016/j.supflu.2011.11.002>.
- [13] El-Maghraby RM, Blunt MJ. Residual CO₂ trapping in Indiana limestone. *Environ Sci Technol* 2013;47(1):227–33. <http://dx.doi.org/10.1021/es304166u>.
- [14] Fernø MA, Torsvik M, Haugland S, Graue A. Dynamic laboratory wettability alteration. *Energy Fuels* 2010;24:3950–8. <http://dx.doi.org/10.1021/ef1001716>.
- [15] Geffen TM, Parrish DR, Haynes GW, Morse RA. Efficiency of gas displacement from porous media by liquid flooding. *J Pet Technol* 1952;4:29–38. <http://dx.doi.org/10.2118/952029-G>.

- [16] Graue A, Viksund BG, Eilertsen T, Moe R. Systematic wettability alteration by aging sandstone and carbonate rock in crude oil. *J Pet Sci Eng* 1999;24:85–97. [http://dx.doi.org/10.1016/S0920-4105\(99\)00033-9](http://dx.doi.org/10.1016/S0920-4105(99)00033-9).
- [17] Humphry KJ, Suijkerbuijk BMJM, van der Linde HA, Pieterse SGJ, Masalmeh SK. Impact of wettability on residual oil saturation and capillary desaturation curves. In: *Proceedings of society of core analysts held in Napa Valley, California, USA, SCA2013-025*; 2013.
- [18] Jadhunandan PP, Morrow NR. Effect of wettability on waterflood recovery for crude-oil/brine/rock systems. *SPE Reserv Eng* 1995;10:40–6. <http://dx.doi.org/10.2118/22597-PA>.
- [19] Johannessen EB, Graue A. Mobilization of remaining oil – emphasis on capillary number and wettability. In: *Proceedings of international oil conference and exhibition in Mexico*, 27–30 June, SPE-108724-MS; 2007. <http://dx.doi.org/10.2118/108724-MS>.
- [20] Karabakal U, Bagci S. Determination of wettability and its effect on waterflood performance in limestone medium. *Energy Fuels* 2004;18(2):438–49. <http://dx.doi.org/10.1021/ef030002f>.
- [21] Kovscek AR, Wong H, Radke CJ. A pore-level scenario for the development of mixed wettability in oil reservoirs. *Environ Energy Eng* 1993;39:1072–85. <http://dx.doi.org/10.2118/24880-MS>.
- [22] Krevor SC, Pini MR, Li B, Benson SM. Capillary heterogeneity trapping of CO₂ in a sandstone rock at reservoir conditions. *Geophys Res Lett* 2011;38:L15401. <http://dx.doi.org/10.1029/2011GL048239>.
- [23] Krevor SCM, Blunt MJ, Benson SM, Pentland CH, Reynolds C, Al-Menhali A, et al. Capillary trapping for geologic carbon dioxide storage from pore scale physics to field scale implications. *Int J Greenh Gas Control* 2015;40:221–37. <http://dx.doi.org/10.1016/j.ijggc.2015.04.006>.
- [24] Lake LW. *Enhanced oil recovery*. Old Tappan, NJ: Prentice Hall Inc.; 1989.
- [25] Land CS. Comparison of calculated with experimental imbibition relative permeability. *SPE J* 1971;11:419–25. <http://dx.doi.org/10.2118/3360-PA>.
- [26] Lenormand R, Zarcone C, Sarr A. Mechanisms of the displacement of one fluid by another in a network of capillary ducts. *J Fluid Mech* 1983;135:337–53. <http://dx.doi.org/10.1017/S0022112083003110>.
- [27] Lenormand R, Zarcone C. Role of roughness and edges during imbibition in square capillaries. In: *Proceedings of SPE annual technical conference and exhibition*, 16–19 September, Houston, Texas, SPE-13264-MS; 1984. <http://dx.doi.org/10.2118/13264-MS>.
- [28] Ma TD, Youngren GK. Performance of immiscible water-alternating-gas (IWAG) injection at Kuparuk river unit north slope Alaska. In: *Proceedings of the SPE annual technical conference and exhibition*, New Orleans, Louisiana, 25–28 September, SPE 28602-MS; 1994. <http://dx.doi.org/10.2118/28602-MS>.
- [29] Masalmeh SK. High oil recoveries from transition zones. In: *Proceedings of the Abu Dhabi international petroleum exhibition and conference*, SPE-87291-MS; 2000. <http://dx.doi.org/10.2118/87291-MS>.
- [30] Masalmeh SK, Oedai S. Oil mobility in transition zone. In: *Proceedings of society of core analysts held in Abu Dhabi, UAE, SCA2000-02*; 2000. <http://dx.doi.org/10.2118/87291-MS>.
- [31] Masalmeh SK. The effect of wettability on saturation functions and impact on carbonate reservoirs in the middle east. In: *Proceedings of the Abu Dhabi international petroleum exhibition and conference*, SPE-78515-MS; 2002. <http://dx.doi.org/10.2118/78515-MS>.
- [32] Masalmeh SK. Impact of capillary forces on residual oil saturation and flooding experiments for mixed to oil-wet carbonate reservoirs. In: *Proceedings of society of core analysts held in Aberdeen, Scotland, UK, SCA2012-11*; 2012.
- [33] Morrow NR. The effects of surface roughness on contact: angle with special reference to petroleum recovery. *J Can Pet Technol* 1975;14. <http://dx.doi.org/10.2118/75-04-04>.
- [34] Muir-wood HM. Some jurassic brachiopoda from the Lincolnshire limestone and upper estuarine series of rutland and Lincolnshire. *Proc Geol Assoc* 1952;63:113–42. [http://dx.doi.org/10.1016/S0016-7878\(52\)80014-8](http://dx.doi.org/10.1016/S0016-7878(52)80014-8).
- [35] Nono F, Bertin H, Hamon G. Oil recovery in the transition zone of carbonate reservoirs with wettability change: hysteresis models of relative permeability versus experimental data. In: *Proceedings of society of core analysts held in Avignon, France, SCA2014-007*; 2014.
- [36] Øren P, Bakke S. Process based reconstruction of sandstones and prediction of transport properties. *Transp Porous Media* 2002;46:311–43. <http://dx.doi.org/10.1023/A:1015031122338>.
- [37] Pentland CH, Itsekiri E, Al-Mansoori S, Iglauer S, Bijeljic B, Blunt MJ. Measurement of nonwetting-phase trapping in sandpacks. *SPE J* 2010;15:274–81. <http://dx.doi.org/10.2118/115697-PA>.
- [38] Pentland CH, Tanino Y, Iglauer S, Blunt MJ. Residual saturation of water-wet sandstones: experiments, correlations and pore-scale modeling. In: *Proceedings of the SPE annual technical conference and exhibition*, Florence, Italy, SPE 133798; 2010. <http://dx.doi.org/10.2118/133798-MS>.
- [39] Pentland CH, El-Maghraby R, Iglauer S, Blunt MJ. Measurements of the capillary trapping of super-critical carbon dioxide in berea sandstone. *Geophys Res Lett* 2011;38:L06401. <http://dx.doi.org/10.1029/2011GL046683>.
- [40] Rezaei N, Firoozabadi A. Pressure evolution and production performance of waterflooding in n-heptane-saturated fired berea cores. *SPE J* 2014;19:674–86. <http://dx.doi.org/10.2118/167264-PA>.
- [41] Roof JG. Snap-off of oil droplets in water-wet pores. *Soc Pet Eng J* 1970;10:85–90. <http://dx.doi.org/10.2118/2504-PA>.
- [42] Ryazanov AV, van Dijke M, Sorbie KS. Two-phase pore-network modelling: Existence of oil layers during water invasion. *Transp Porous Media* 2009;80:79–99. <http://dx.doi.org/10.1007/s11242-009-9345-x>.
- [43] Salathiel RA. Oil recovery by surface film drainage in mixed-wettability rocks. *J Pet Technol* 1973;25:1216–24. <http://dx.doi.org/10.2118/4104-PA>.
- [44] Skauge A, Sørvik A, Vik B, Spildo K. Effect of wettability on oil recovery from carbonate material representing different pore classes. In: *Proceedings of society of core analysts held in Trondheim, Norway, SCA2006-01*; 2006.
- [45] Tang G, Firoozabadi A. Effect of pressure gradient and initial water saturation on water injection in water-wet and mixed-wet fractured porous media. *SPE Reserv Eval Eng* 2001;4:516–24. <http://dx.doi.org/10.2118/74711-PA>.
- [46] Tanino Y, Blunt MJ. Capillary trapping in sandstones and carbonates: dependence on pore structure. *Water Resour Res* 2012;48:W08525. <http://dx.doi.org/10.1029/2011WR011712>.
- [47] Tanino Y, Blunt MJ. Laboratory investigation of capillary trapping under mixed-wet conditions. *Water Resour Res* 2013;49:4311–19. <http://dx.doi.org/10.1002/wrcr.20344>.
- [48] Tie H, Morrow NR. Oil recovery by spontaneous imbibition before and after wettability alteration of three carbonate rocks by a moderately asphaltic crude oil. In: *Proceedings of society of core analysts held in Toronto, Canada, SCA2005-11*; 2005.
- [49] Valvatne PH, Blunt MJ. Predictive pore-scale modeling of two-phase flow in mixed wet media. *Water Resour Res* 2004;40:W07406. <http://dx.doi.org/10.1007/s11242-009-9345-x>.
- [50] Vincent JV, Kilpatrick PK. Preferential solvent partitioning within asphaltic aggregates dissolved in binary solvent mixtures. *Energy Fuels* 2007;21:1217–25. <http://dx.doi.org/10.1021/ef060456n>.
- [51] Watson J. *British and foreign building stones: a descriptive catalogue of the specimens in the sedgwick museum*. Cambridge, UK: Cambridge University Press; 1911.
- [52] Wu Y, Shuler PJ, Blanco M, Tang Y, Goddard WA. An experimental study of wetting behavior and surfactant EOR in carbonates with model compounds. *SPE J* 2008;13:26–34. <http://dx.doi.org/10.2118/99612-PA>.
- [53] Zhou X, Morrow NR, Ma S. Interrelationship of wettability, initial water saturation, aging time, and oil recovery by spontaneous imbibition and waterflooding. *SPE J* 2000;5:199–207. <http://dx.doi.org/10.2118/62507-PA>.